

©Prof. Roger G. Mark, 2004

MASSACHUSETTS INSTITUTE OF TECHNOLOGY

Departments of Electrical Engineering, Mechanical Engineering,
and the Harvard-MIT Division of Health Sciences and Technology

6.022J/2.792J/HST542J: Quantitative Physiology: Organ Transport Systems

PRINCIPLES OF CARDIAC ELECTROPHYSIOLOGY

- I. Electrophysiology of Myocardial Cells
- II. The Physical Basis of Electrocardiography

Text Reference: pages 115-126

TABLE OF CONTENTS

INTRODUCTION.....	1
1. ELECTROPHYSIOLOGY OF MYOCARDIAL CELLS	1
1.1 The Cardiac Action Potential.....	1
1.2 The Ionic Basis for the Cellular Potentials.....	2
1.2.1 Phase 4 - Resting Potential	5
1.2.2 Phase 0 - Depolarization.....	5
1.2.3 Phase 1 - Repolarization	9
1.2.4 Phase 2 - Plateau.....	9
1.2.5 Phase 3 - Repolarization	9
1.3 Propagation of the Action Potential.....	9
1.3.1 The Cable Model	12
1.4 Automaticity.....	15
1.5 Excitability.....	19
1.5.1 Cells with Fast Channels.....	19
1.5.2 Cells with Slow Response	21
1.6 Interval-Duration Relationship.....	21
1.7 Excitation-Contraction Coupling.....	22
1.8 The Cardiac Conduction System	23
2. THE PHYSICAL BASIS OF ELECTROCARDIOGRAPHY	28
2.1 Introduction	28
2.2 The Dipole Model.....	29
2.2.1 The Source.....	29
2.2.2 Electrical Properties of Tissue.....	33
2.2.3 Calculation of Potential within the Sphere.....	35
2.2.4 The Surface Potentials	36

2.3 Lead Systems Used in Scalar Electrocardiography	39
2.3.1 Frontal Plane Scalar Leads.....	40
2.3.2 Precordial Leads	42
2.4 Electrical Axis	44

PRINCIPLES OF CARDIAC ELECTROPHYSIOLOGY

INTRODUCTION

The heart's pumping action depends on the rhythmic, coordinated contraction of the ventricles and the proper functioning of the valves. Each mechanical heartbeat is triggered by an action potential which originates from a rhythmic, pacemaker cell within the heart. The impulse is then conducted rapidly throughout the organ in order to produce coordinated contraction.

Disturbances in the heart's electrical activity may cause significant abnormalities in its mechanical function, and are the basis of much cardiac morbidity and mortality. In fact, malfunction of the heart's electrical behavior is the principal cause of sudden cardiac death. This chapter will discuss cardiac electrophysiology beginning at the cellular level. We will then explore the anatomy and electrophysiology of the cardiac conduction system, and the normal sequence of myocardial depolarization. Finally, we will relate the electrical activity of the myocardium to body surface potentials using the simple dipole model.

ELECTROPHYSIOLOGY OF MYOCARDIAL CELLS

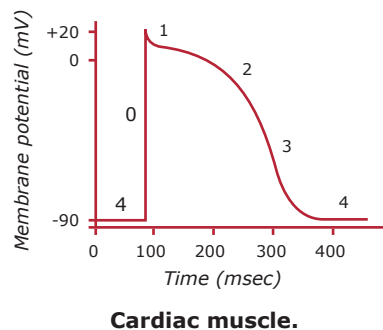
1.1 The Cardiac Action Potential

Cardiac transmembrane potentials may be recorded by means of microelectrodes. A typical resting potential in a ventricular muscle fiber is -80 to -90 millivolts with respect to surrounding extracellular fluid, similar to that found in nerve and skeletal muscle. The shape of the cardiac action potential, however, is quite distinctive primarily because of its long duration. A typical action potential from a ventricular cell is diagrammed in Fig. 1. Its total duration may be 200-300 milliseconds (in contrast to 1 or 2 milliseconds for nerve and skeletal muscle), and it consists of 5 distinct phases. The initial rapid upstroke (phase 0) from the resting potential to a positive value of about +20 millivolts is similar to the spikes of other cells. Early repolarization (phase 1) brings the potential down to a plateau level over 2 to 3 milliseconds. The plateau itself (phase 2) follows, and

accounts for most of the action potential duration. Repolarization (phase 3) brings the potential back to the resting level. The period between action potentials (phase 4) is stable except in cells which have the property of autorhythmicity, which will be discussed later.

A cardiac action potential, once started in a cell, propagates by local current spread as in other excitable cells.

Figure 1 - A Typical Action Potential from a Ventricular Myocardial Cell



Cardiac muscle.

Figure by MIT OCW.

1.2 The Ionic Basis for the Cellular Potentials

The ionic basis for the cardiac action potential has features which are similar to those of nerve and skeletal muscle (Katz, 1966), but there are important differences also (Noble, 1979). Cardiac cells maintain gradients of various ions across their membranes by energy-requiring pumps. Table 1 shows representative concentrations of several important ionic species for the cat heart.

Table 1 - Ion Concentrations and Equilibrium Potentials in Cat Heart
 (From Honig, Carl R., Modern Cardiovascular Pathophysiology, Little Brown and Co., 1981, p. 18)

Ion	Concentrations (MEq/L)		Equilibrium Potential (mV)
	Outside	Inside	
Na ⁺	145	32	+40
K ⁺	5.3	172	-90
Ca ⁺⁺	5.2	.00007*	+205
Cl ⁻	87	30	-28

*Ca⁺⁺ is too low to measure. Value shown is in the range required to prevent interaction of actin and myosin.

The cell membrane is semi-permeable, and contains a number of functionally independent “channels” through which different ions flow.

Fig. 2 is a circuit representation of a unit area of cell membrane showing channels for the important ionic species of sodium, potassium, and calcium. The fourth pathway represents all other ionic species. Each channel has a specific ionic conductance (which may vary with membrane potential or time) and an equilibrium potential for the relevant ion. The membrane capacitance is represented by C_m . The total current density flowing across the membrane is J_m , and in general is carried by a mixture of several ionic species. The overall net transmembrane potential is V_m . The flow of the i^{th} ionic species is determined by the conductivity of its channel, g_i , and its equilibrium potential, V_i which is given by the Nernst equilibrium equation:

$$V_i = \frac{RT}{Z_i F} \ln \frac{\eta_i^{\text{outside}}}{\eta_i^{\text{inside}}} \quad (1)$$

where

R = the gas constant, 8.2 joules/mole degree K

T = the absolute temperature, degrees K

F = Faraday's constant, 9.65×10^4 coul./mole

Z_i = valence of the i^{th} ion

η_i = molar concentration of the i^{th} ion

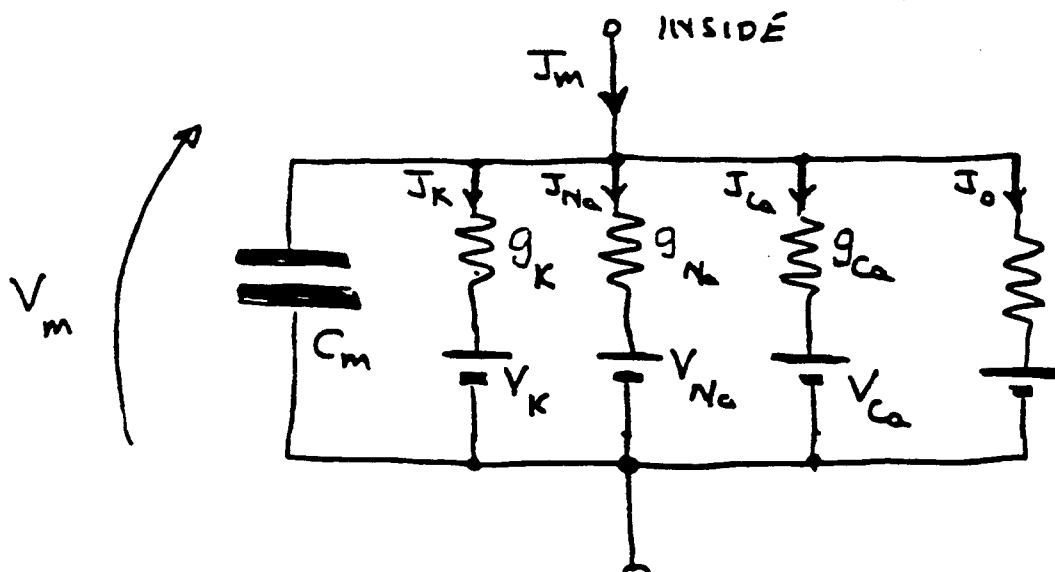
At room temperature, equation (1) becomes approximately

$$V_i = \frac{60}{Z_i} \log_{10} \frac{\eta_i^{\text{outside}}}{\eta_i^{\text{inside}}} \text{ (millivolts)} \quad (2)$$

Table 1 gives typical values of the equilibrium potentials for several important ions.

Individual ions pass through the cell membrane through discrete ionselective channels. The permeability of the channels may be quite different for different ionic species, and in addition the permeability may be changed dramatically as a function of the potential difference across the membrane, or as a result of the activation of membrane receptors.

Figure 2 - Circuit Model of a Unit Area of Cell Membrane



From the circuit of Fig. 2 we have the following expression for the membrane current density J_m :

$$J_m = C_m \frac{dV_m}{dt} + \sum_i g_i (V_m - V_i) \quad (3)$$

where C_m is the membrane capacitance, V_m is the transmembrane potential, and g_i is the membrane conductance for the ionic species, i .

Phase 4 - Resting Potential

The resting potential (phase 4) in non-pacemaker cardiac cells is established by the same mechanisms as for other excitable cells. Referring to the model during the resting state ($dV_m/dt = 0$), and assuming no externally applied current, we have $J_m = 0$. Solving eq. (3) for the resultant potential, we have

$$V_m^0 = \frac{g_K}{g_m} V_K + \frac{g_{Na}}{g_m} V_{Na} + \frac{g_{Ca}}{g_m} V_{Ca} + \frac{g_0}{g_m} V_0 \quad (4)$$

where

$$g_m = \sum_i g_i$$

and V_m^0 is the resting potential. In the resting state the cell membrane is much more permeable to potassium than to the other ions, hence $gK/g_m \approx 1$. As a result, the resting potential is close to V_K : typically -80 to -90 mV in ventricular myocardial cells.

1.2.2 Phase 0 — Depolarization

The ionic mechanism underlying phase 0 depolarization in most cardiac muscle cells is similar to that of nerve and skeletal muscle—namely a rapid (and transient) regenerative increase in

sodium conductance, g_{Na} to values almost two orders of magnitude greater than peak g_K or g_{Ca} . This permits the membrane potential to shift toward the sodium equilibrium potential (+40 mV). The fact that the action potential never reaches V_{Na} reflects the residual permeability of the membrane to potassium. It has been shown that phase 0 is also accompanied by a fall in potassium conductance, with much slower kinetics. (See Fig. 3.)

It has been demonstrated that there is a second important inward (depolarizing) current which is activated by depolarization of the cell. This current is not sensitive to variations in extracellular sodium concentration, but is very sensitive to extracellular calcium concentration. The kinetics of this second current are very sluggish, both during activation and inactivation. This so-called “slow inward current” is carried primarily by calcium ions and plays an important role in the activation of mechanical contraction. Most cardiac cells utilize both fast and slow currents. Fig. 4 presents a hypothetical representation of the fast (Na^+) and slow (Ca^{++}) components of the cardiac action potential. (Notice that the slow inward current is the primary determinant of the phase 2 plateau.)

It is possible to selectively disable one or the other of the two inward channels. The sodium channel may be inactivated by partially depolarizing the membrane to about -60 mV. This channel may also be selectively blocked by tetrodotoxin (TTX), a poison derived from the Japanese puffer fish. With the sodium channel blocked, cells will exhibit the slow response only, although sympathomimetic amines such as epinephrine or isoproterenol may be required to stimulate the slow channel sufficiently to generate action potentials. Fig. 5 shows action potentials of the “slow response” type in Purkinje cells whose sodium channels were inactivated by increasing doses of tetrodotoxin (in the presence of epinephrine).

Figure 3 - Changes in ionic conductances during the cardiac action potential.

The typical action potential is shown (top), with the corresponding changes in conductance for potassium (g_K), sodium (g_{Na}), chlorine (g_{Cl}), and calcium (g_{Ca}) (From Katz, 1977).

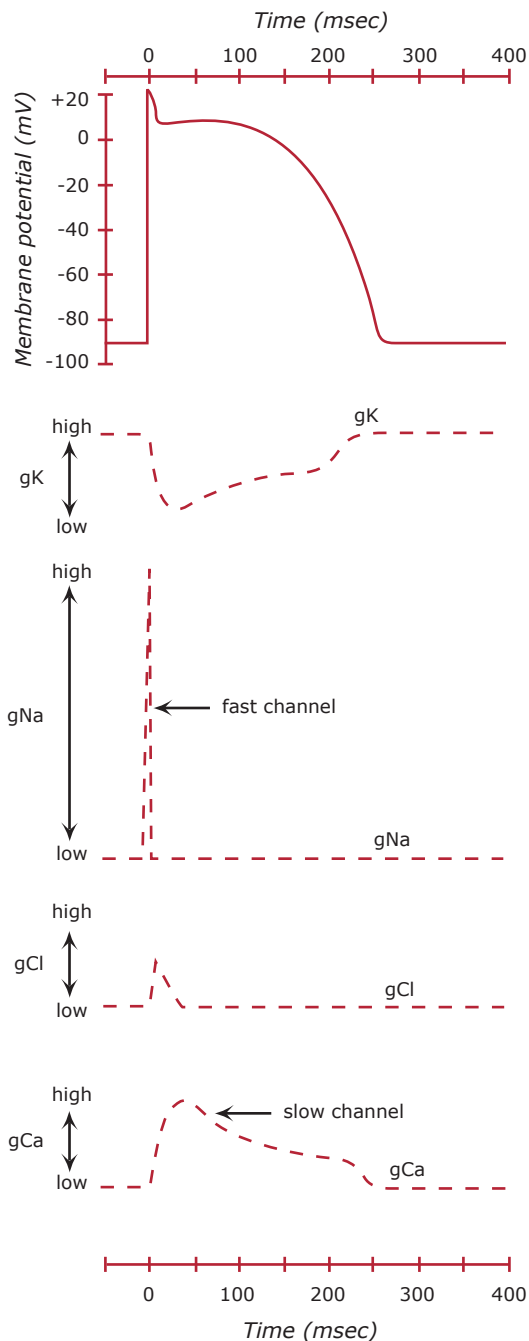
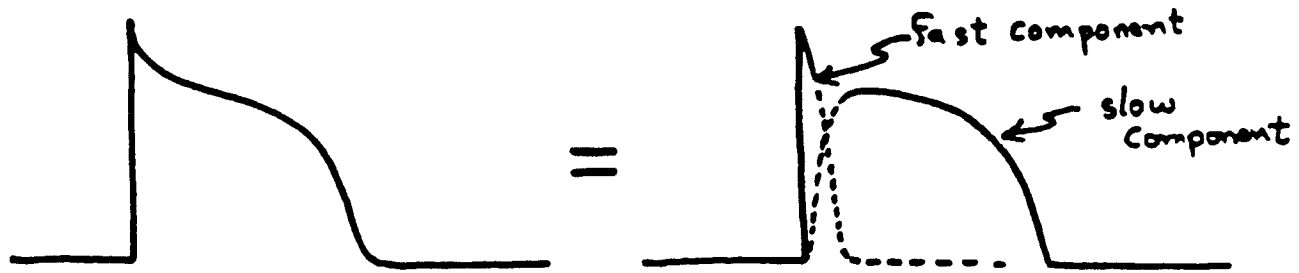


Figure by MIT OCW. After Katz, 1977.

Figure 4 - Diagrammatic representation of the contributions of the fast and slow channels to the action potential.



The slow channels may be specifically blocked by certain drugs (Verapamil, D600) or cations such as manganese, cobalt, or nickel. Such drugs markedly reduce action potential duration, inhibit automaticity in the SA node, and slow conduction in the AV node.

Figure 5 - Progressive blockade of I_{Na^+} in calf Purkinje fiber by increasing doses of tetrodotoxin.

The time course in E resembles action potentials in cells of the SA and AV nodes. The experiment was performed in the presence of epinephrine, which enhances I_{Na^+} . (Modified from E. Carmeliet and J. Vereecke, Pfluegers Arch. 313:303, 1969. From Honig, Carl R., Modern Cardiovascular Physiology 1981, Little Brown & Co., Inc. p. 26.)

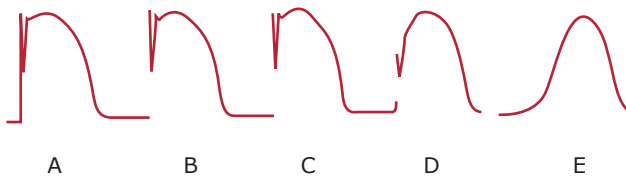


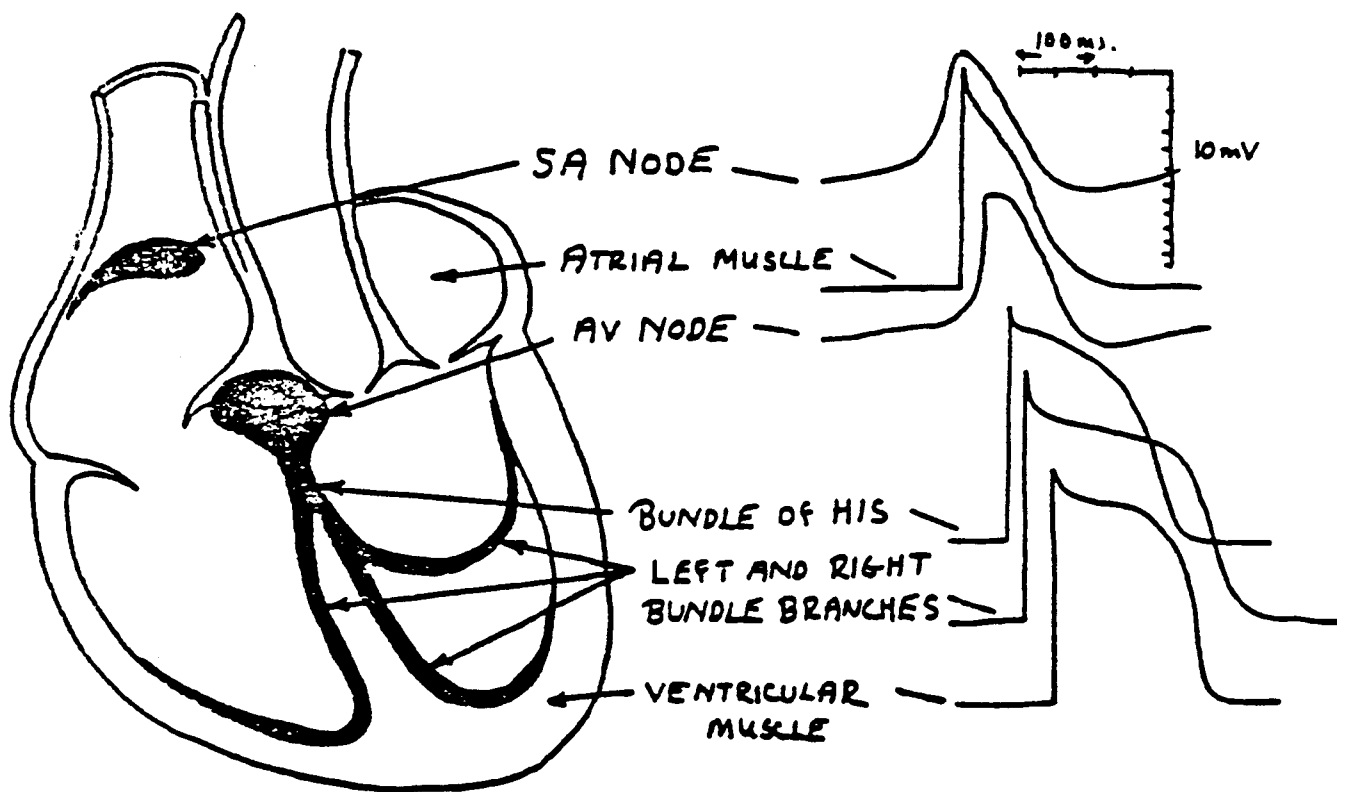
Figure by MIT OCW. After E. Carmeliet and J. Vereecke 1969, cited in Honig, Carl R. *Modern Cardiovascular Physiology*. 1981, Little Brown & Co., Inc. p. 26.

Some cells in the heart appear to lack the fast sodium channels, and function normally with only the slow current mechanism. These cells are located in the sinoatrial (SA) node, and in the atrioventricular (AV) node. Fig. 6 shows transmembrane action potentials from cells at various locations in the heart's conduction system. Notice the SA and AV nodal action potentials: they show the slow rise-time characteristic of the slow current. Their resting potentials are also typically

low, about -60 mV. In addition, these cells conduct the action potential much more slowly (.01 - 0.1 meters/sec) than cells with rapid rise times (0.5 - 3.0 m/s).

Figure 6 - The Cardiac Conduction System

The sketch below demonstrates the major anatomical structures of the conduction system of the heart, with typical transmembrane action potentials shown on right. (Redrawn from Phillips RE, Feeney MK, 1980 The Cardiac Rhythms. Saunders, Philadelphia and from Hoffman BF, Cranefield PF 1960 Electrophysiology of the Heart. McGraw Hill, New York.)



1.2.3 Phase I — Repolarization

Phase 1 repolarization, like that in nerve and skeletal muscle, is due primarily to a fall in sodium conductance. (See Fig. 3.)

1.2.4 Phase 2 — Plateau

The plateau (phase 2) is the most distinctive feature of the cardiac action potential. During the plateau there is an approximate balance between inward-going calcium current and outward-going potassium current, and the membrane conductance is relatively low. The slow calcium current is the principal inward current during the plateau.

1.2.5 Phase 3 — Repolarization

Repolarization (phase 3) is a complex process which is not completely understood. Several mechanisms seem to be important. First, the potassium conductance increases, tending to repolarize the cell via a potassium-mediated outward current. The opening of these potassium channels is both time and voltage dependent: the potassium current increases with time after the peak of the action potential even if V_m is held constant. On the other hand, voltage dependence is shown by the fact that the potassium current can be increased by electrically repolarizing the cell. In addition to the potassium mechanism, there is a time dependent decrease in calcium conductivity which also contributes to cellular repolarization.

1.3 Propagation of the Action Potential

An action potential, once initiated in a cardiac cell, will propagate along the cell membrane until the entire cell is depolarized. Myocardial cells also have the unique property of transmitting action potentials from one cell to adjacent cells by means of direct current spread (without electrochemical synapses). In fact, until about 1954 there was almost general agreement that the myocardium was an actual syncytium without separate cell boundaries. But the electron microscope identified definite cell membranes, showing that adjacent cells are separated by an extracellular space of variable width. Cells join along structures known as intercalated disks (Fig. 7). The location of the low resistance connection between cells is a part of the intercalated disk known as the gap junction or nexus. Ionic currents flow from cell to cell via these intercellular connections, and the heart behaves electrically as a functional syncytium. Thus, an impulse originating anywhere in the myocardium will propagate throughout the heart, resulting in a coordinated mechanical

contraction. (The atria, however, are electrically insulated from the ventricles except for the AV node.) An artificial cardiac pacemaker, for example, introduces depolarizing electrical impulses via an electrode catheter usually placed within the right ventricle. Pacemaker-induced action potentials excite the entire ventricular myocardium resulting in effective mechanical contractions.

Figure 7 - The Intercalated Disk

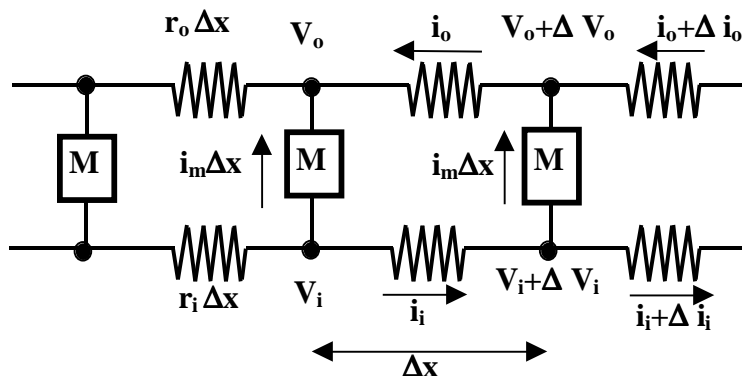
Image removed due to copyright considerations.

Electron microphotographs of the intercalated disc. **Top:** Transverse section of cat ventricular myocardium, showing insertions of thin filaments into filamentous mats (*arrows*), which bind to the intercalated disc to form the fascia adherens (FA). This intracellular junction changes form at the *right* of the figure, where the two cells come into contact at a nexus, or gap junction (N). **Bottom:** Oblique section of intercalated disc in mouse ventricular myocardium, showing filaments (*arrow*) joining fascia adherens (FA) and a nexus (N). Two maculae adherens (MA), or desmosomes, are also shown. All of these structures represent specialized cell-cell junctions. (From McNutt and Fawcett (1974), courtesy of Wiley, New York.)

1.3.1 — The Cable Model

How is an action potential propagated along a cell? The one-dimensional cable model of the cell is helpful in understanding the process. The cardiac cell may be thought of as a cylindrical membrane which separates the internal conducting medium from the extracellular conducting medium. The membrane may be considered as a relative insulator with properties described in previous sections. Fig. 8 is a schematic diagram of the model, which assumes that charge carriers are restricted to move in only one dimension inside and outside of the cell. The boxes, M, represent the lumped properties of the membrane over a length of Δx . The resistances per unit length of the inside and outside conductors are r_i and r_o respectively; i_m represents the transmembrane current per unit length.

Figure 8 - The Cable Model of a Cylindrical Cell



The currents flowing inside and outside of the cell are i_i and i_o , and at any particular point they must be equal and opposite, since there are no current sources or sinks, or other available current paths. V_o and V_i represent the extracellular and intracellular potentials, respectively. The transmembrane potential V_m is $(V_i - V_o)$ at each position along the cell. All currents and voltages are, in general, functions of both position and time.

By applying Ohm's law, we have:

$$i_i r_i \Delta x = -\Delta V_i \quad (5)$$

In the limit as $\Delta x \rightarrow 0$ this becomes:

$$\frac{\partial V_i}{\partial x} = -i_i r_i \quad (6)$$

By similar reasoning applied to the outer conductor, we obtain

$$\frac{\partial V_o}{\partial x} = i_o r_o = i_i r_o \quad (7)$$

By analyzing current flows at any node, we observe that

$$\Delta i_i = -i_m \Delta x \quad (8)$$

or in the limit:

$$\frac{\partial i_i}{\partial x} = -i_m \quad (9)$$

Recalling the definition of V_m , and using (6) and (7)

$$\begin{aligned} \frac{\partial V_m}{\partial x} &= \frac{\partial}{\partial x} (V_i - V_o) = \frac{\partial V_i}{\partial x} - \frac{\partial V_o}{\partial x} = -i_i (r_i + r_o) \\ i_i &= -\frac{1}{(r_i + r_o)} \frac{\partial V_m}{\partial x} \end{aligned} \quad (10)$$

Differentiating and substituting into (9) we obtain

$$i_m = \frac{1}{(r_i + r_o)} \frac{\partial^2 V_m}{\partial x^2} \quad (11)$$

The membrane current per unit length is given by:

$$i_m = C_m \frac{\partial V_m}{\partial t} + \frac{V_m}{r_m} \quad (12)$$

where C_m is the membrane capacitance per unit length and r_m is the equivalent membrane resistance per unit length. Substituting equation (12) into equation (11) results in the differential equation:

$$\frac{\partial^2 V_m(x,t)}{\partial x^2} = (r_o + r_i) \left[C_m \frac{\partial V_m}{\partial t} + \frac{V_m}{r_m} \right] \quad (13)$$

1.3.1.1 The Space Constant

This equation may be solved simply for the time invariant case $\left(\frac{\partial V_m}{\partial t} = 0 \right)$ to yield the variation of membrane potential with length resulting from a fixed initial transmembrane potential V_0 at one point ($x=0$) on an infinitely long strip of muscle cells.

$$V_m(x) = V_0 e^{-x/\lambda} \quad (14)$$

where $\lambda = \sqrt{\frac{r_m}{r_i + r_o}}$.

The membrane current, i_m , will have the same functional form as V_m . λ is the so-called “space constant,” and is a measure of the distance from the origin at which the membrane potential (or current) falls to $1/e$ of its initial value.¹

¹ r_m , r_i , r_o have been defined in terms associated with a particular cell. In order to account for geometric factors, it is useful to use units for conductivities which are geometry-independent. We will also simplify the expressions by assuming that $r_o \ll r_i$.

Define: $r_i = \frac{r}{\pi a^2}$ where ρ is the resistivity ($\Omega - c_m$) of the internal media.

$r_m = \frac{R_m}{2\pi a}$ where R_m is the transverse membrane resistivity in $\Omega - c_m^2$.

$c_m = 2\pi a C_m$ where C_m = capacitance per unit area

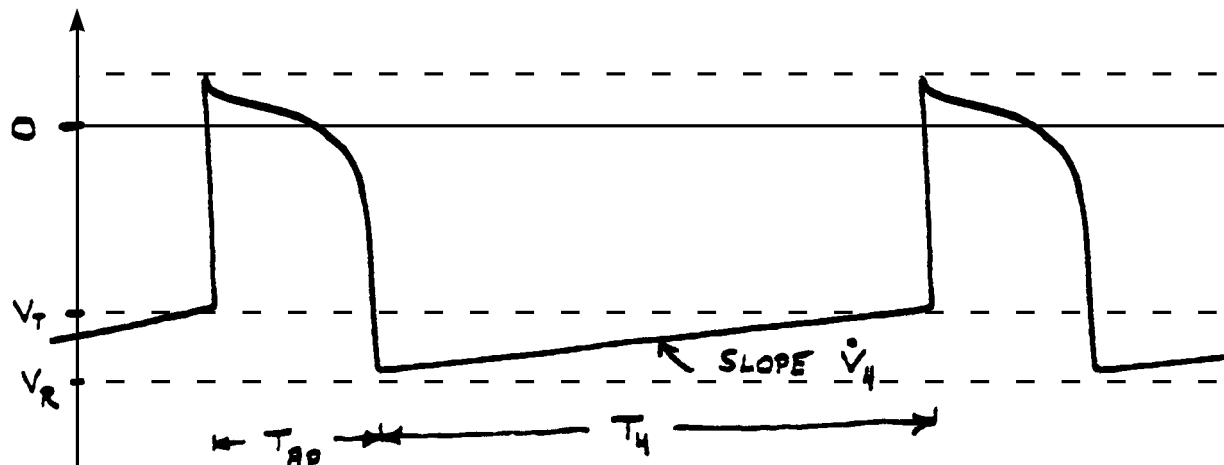
It follows that $\lambda = \sqrt{\frac{a R_m}{2\rho}}$.

The transmembrane current depolarizes the membrane ahead of the action potential, and thereby propagates the impulse down the cell. The current also flows from one cell to the next via the low-resistance nexi, and thus the action potential spreads directly from cell to cell. The velocity of propagation increases with increasing cell diameter, action potential amplitude, and the initial rate of the rise of the action potential. The resistance of the nexi also has a major impact on conduction velocity: increased resistance slows conduction velocity.

1.4 Automaticity

A number of cardiac cells display the property of automaticity — that is, they have the ability to spontaneously generate propagated action potentials, and function as pacemaker cells. Such cells are found in the SA node, the specialized conduction systems of the atria and ventricles, and in the AV nodal region. In automatic cells, the diastolic (phase 4) potential is not stable, but shows spontaneous depolarization (Fig. 9).

Figure 9
Diagram of the Transmembrane Potential of an Automatic Cell



Notice that the membrane potential starts at the resting potential, V_R , and that it slowly increases toward zero. When the potential reaches a threshold level, V_T , the cell develops an action potential. Following the action potential, the membrane potential returns to the resting level and the cycle repeats.

Spontaneous phase 4 depolarization occurs in cells with high levels of membrane potential (-60 to -90 mV), and also in cells with low membrane resting potentials (≥ -60 mV). The former group includes cells in the Purkinje system and cells of the atrial conduction system. The second group includes cells in the SA node, the AV junction and Purkinje fibers which have been partially depolarized experimentally or by local pathology. The mechanism underlying phase 4 depolarization is probably different in the two groups of cells. Phase 4 depolarization in the first group is thought to be due to a spontaneous decrease in potassium conductance, g_K , during diastole in the presence of a steady inward sodium movement. The result is a movement of the membrane potential toward the sodium equilibrium potential. When threshold is reached, these cells develop an action potential with a rapid upstroke (Fig. 10).

Figure 10
Automatic Activity in Purkinje fibers (in the presence of 0.1 mm barium chloride in Tyrode's solution). Calibration: vertical, 25mV, horizontal 20 msec.

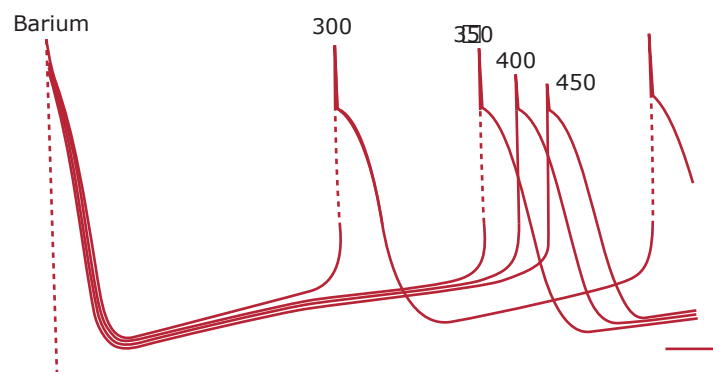


Figure by MIT OCW.

For automatic cells with low membrane resting potentials, the sodium channels are inactivated, and the mechanisms underlying phase 4 depolarization are not so clear. Spontaneous

impulse generation does occur, and is presumably the normal mechanism for SA nodal activity. (See Fig. 11.) The action potentials have the slow upstroke characteristic of the slow current mechanism. It appears that the slow inward current may underlie automaticity in these cells. For example, it has been shown that slow-channel blocking agents such as verapamil will reduce the spontaneous rate of the SA node fibers. The effect can be overcome by sympathomimetic amines (such as isoproterenol) which are known to stimulate slow inward current.

Figure 11
Spontaneous Activity in a Single Sinoatrial Node Cell (From Rosen MR, Janse MJ, and Wit AL (eds.): *Cardiac Electrophysiology: A Textbook*. Mount Kisco NY, Futura Publishing Co., 1990, p 119.)

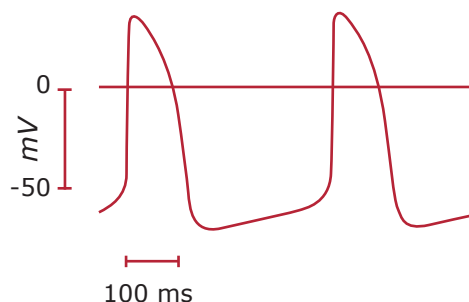


Figure by MIT OCW. After Rosen MR, Janse MJ, and Wit AL (eds.): *Cardiac Electrophysiology: A Textbook*. Mount Kisco NY, Futura Publishing Co., 1990, p. 119.

There is a gradient of automaticity in the heart. The intrinsic rate of the SA node is highest (about 60 per minute), followed by the AV node (about 50 per minute), and the ventricular muscle (about 30-40 per minute). Normally the SA node determines heart rate, the lower pacemakers being reset during each cardiac cycle. However, in some pathologic circumstances, the rate of lower pacemakers can exceed that of the SA node, and then the lower pacemakers determine overall heart rate.

The intrinsic rate of a pacemaking cell can be markedly altered by changing its ionic environment, and by autonomic nervous stimulation. Changes in rate may be mediated by changes in resting potential, threshold potential, or rate of phase 4 depolarization. For example, in Fig. 12 below it is shown that vagal stimulation in the frog sinus venosus reduces the rate of diastolic depolarization and hyperpolarizes the cell, thereby slowing the rate. Vagal stimulation also shortens

action potential duration (Fig. 13). Sympathetic stimulation increases the rate of phase 4 depolarization in both types of automatic cells thus increasing heart rate (Fig. 14).

Figure 12 - Vagal Slowing of Heart Rate

Transmembrane potentials recorded from the frog sinus venosus during vagal stimulation indicated by interruption in horizontal line). (From Butter and Trautwein, 1956.)



Figure by MIT OCW. After Butter and Trautwein, 1956.

Figure 13 - Vagal Effects on Action Potential Duration

Transmembrane action potentials recorded from a single fiber of in situ dog atrium prior to and during vagal stimulation. Top trace is line of zero potential and shows time marks at intervals of 10 and 50 msec. Note progressive decrease in the duration of the action potential and absence of appreciable changes in resting potential or reversal. (Hoffman & Suckling, 1953).

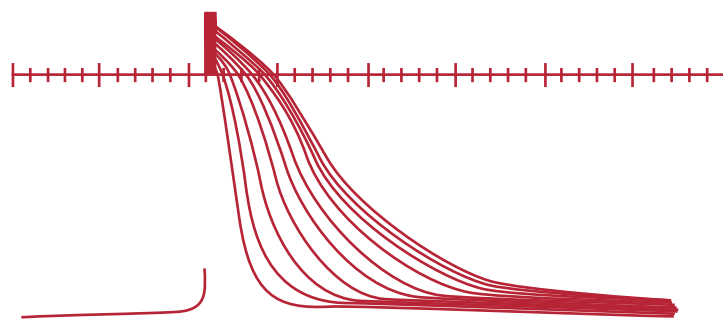


Figure by MIT OCW. After Hoffman and Suckling, 1953.

Figure 14 - Sympathetic Acceleration of Heart Rate

Acceleration of pacemaker activity by sympathetic nerve stimulation and by adrenaline. ~a) Frog sinus venosus. The sympathetic nerve was stimulated during break in horizontal line. (Hutter and Trautwein 1956.) (b) Sheep Purkinje fibre before and after application of adrenaline (Otsuka 1958).

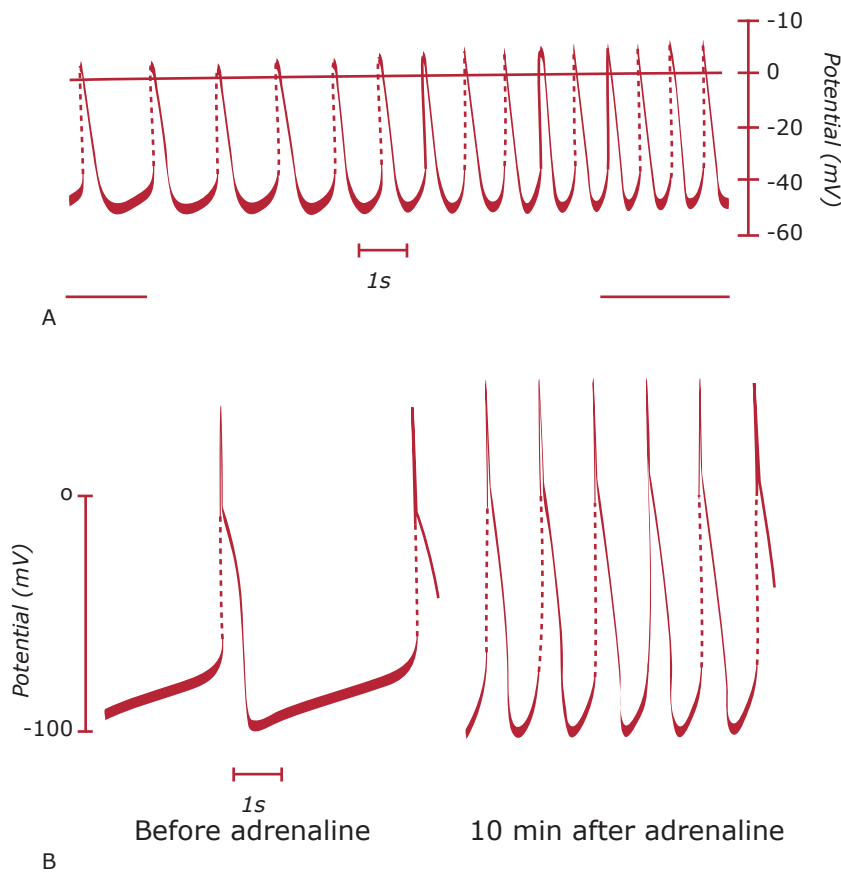


Figure by MIT OCW. After Otsuka 1958.

1.5 Excitability

1.5.1 Cells with Fast Channels

If the transmembrane potential of a resting cell is raised to the threshold potential, V_T , a propagated action potential with a fast rise-time will usually result. The transmembrane potential may be increased to threshold by spontaneous phase 4 depolarization, by electronic spread from adjacent cells, or by external stimulating electrodes. Mechanical deformation may also elicit action potentials.

During a period immediately following an action potential, the cell cannot be re-excited to produce a propagated action potential. This period includes phases 0,1,2, and the first part of phase 3, and is termed the “effective refractory period”. (See Fig. 15.)

Figure 15 - Cellular Excitability

Relationship between transmembrane action potential from single ventricular muscle fiber and excitability of fiber to cathodal stimulation. FRT, Full recovery time; ARP-ERP, effective refractory period; RRP, relative refractory period; SNP, supernormal period. (From Hoffman and Cranefield.)

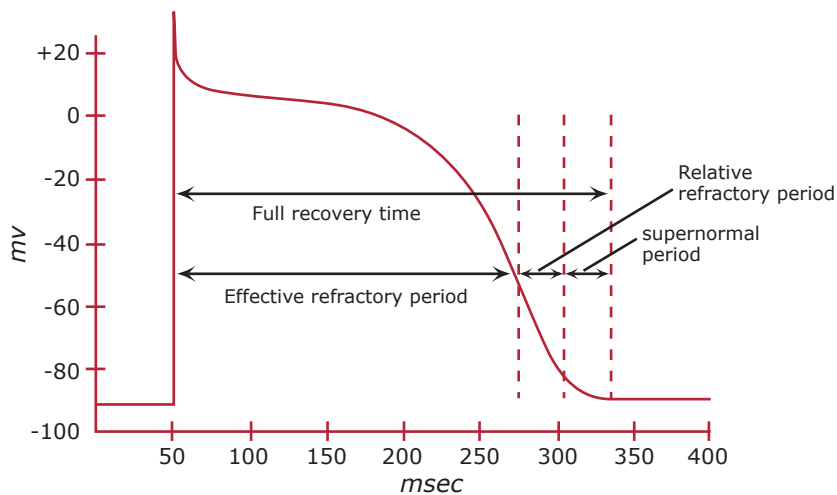


Figure by MIT OCW. After Hoffman and Cranefield.

As the cell begins to repolarize to about -50 mV, it enters the so-called “relatively refractive” period when a propagated action potential can be initiated, but requires a stimulus much stronger than that needed for the resting cell. Furthermore, the resultant action potential is generally of low amplitude, with a slow rise-time and has a slow propagation velocity. (The fast sodium channels are inactivated.) A “supernormal period” follows the relative refractory period. During this time, the cell may be re-triggered with a stimulus slightly smaller than the normal phase 4 threshold stimulus. Thus, excitability is somewhat enhanced. However, the resulting action potential is still somewhat reduced from normal in amplitude, rise-time, and propagation velocity. (The sodium channels are still not fully activated.) In general, the later the second stimulus comes, the more the sodium channels are reactivated, and the more rapid the upstroke of the second action potential (Fig. 16).

Figure 16 - Excitability as a Function of Latency

The changes in action potential amplitude and shape of the upstroke as action potentials are initiated at different stages of the relative refractory period of the preceding excitation. (Redrawn from Rosen, M.S., Wit, A.L., and Hoffman, B.F., Am. Heart J.) 88:380, 1974.)

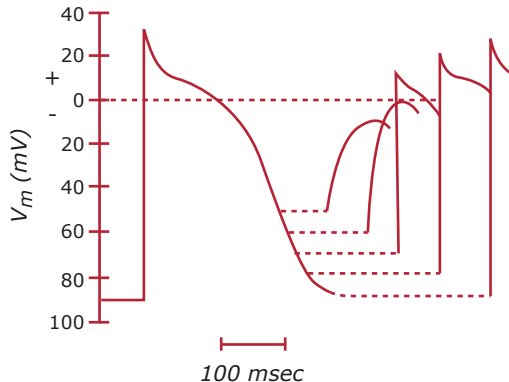


Figure by MIT OCW. After Rosen, M.S., Wit, A.L., and Hoffman, B.F. *Am. Heart J.* 88: 380, 1974.

1.5.2 - Cells with Slow Response

Excitability of the slow response is more complex. The effective refractory period usually extends well beyond the end of phase 3 into phase 4. The recovery of full excitability takes considerably more time (seconds) than for the fast response cells (tenths of seconds). Until full recovery occurs, the conduction velocity varies with excitability. The long refractory periods in these cells account for the development of conduction blocks at the AV junction as heart rate increases. Some fibers showing slow response action potentials seem to demonstrate a cumulative loss of excitability if they are driven too rapidly (manifested clinically as rate-dependent block).

1.6 Interval-Duration Relationship

The duration of the action potential varies with the cycle length (the interval between successive beats). Action potentials following a short interval are shorter in duration, and vice versa (See Fig. 17.) The refractory period is related to the duration of the action potential. Thus, a long pause between two beats will prolong the refractory period of the second beat. This fact is well known in clinical electrocardiography since it explains the tendency for premature impulses following long pauses to find the conduction system in a partially refractive state, resulting in aberrant conduction of these impulses to the ventricles (Ashman phenomenon).

Figure 17 - Interval-Duration relationship

At slow heart rates (A), where the diastolic interval is long, the action potential duration is long. Where the diastolic interval is short, the action potential duration is also short (B). When the heart rate is variable (C), the action potential duration is directly proportional to the duration of the preceding diastolic interval. The lengths of the refractory periods in these beats are closely correlated to the durations of the action potentials.

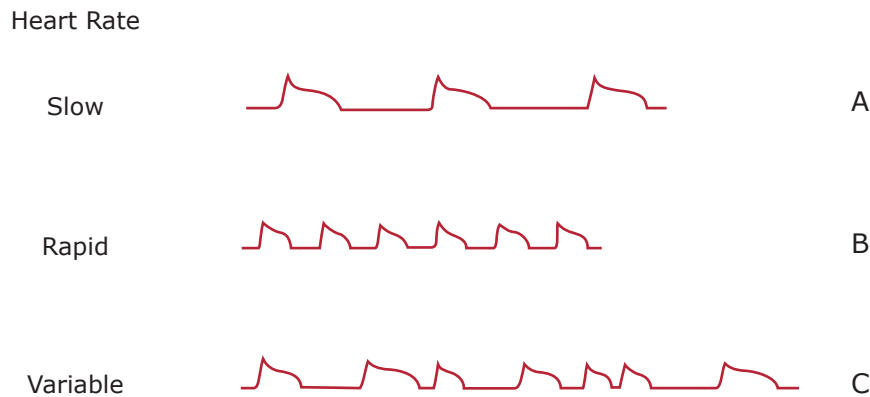


Figure by MIT OCW.

1.7 Excitation-Contraction Coupling

As a wave of electrical depolarization spreads over a myocardial fiber, mechanical contraction is initiated. The relative time courses of the transmembrane potential and the development of isometric force are diagrammed in Fig. 18. Notice that the peak force is developed before the end of the effective refractory period. Cardiac muscle, therefore, cannot be tetanized as can skeletal muscle.

The details of excitation-contraction coupling are quite complex, and are beyond the scope of these notes. In very general terms, the depolarization of the cell membrane is associated with an influx of calcium ions into the cell both from the extracellular sources and from intracellular stores. The calcium ion is released into the vicinity of the sarcomere where it inhibits an inhibitor (troponine-tropomyosin) of the actin-myosin reaction, thus triggering a mechanical contraction (Katz, 1992).

Figure 18 - Electrical and Mechanical Activity in the Myocyte

Diagram showing relationship between transmembrane action potential, A, and isometric tension nerve, B, as recorded from small segment of isolated papillary muscle of cat. Note that peak of isometric tension curve is passed before end of effective refractory period, ERP, of muscle fiber membrane RRP, Relative Refractory Period. (Modified from Brooks et al.)

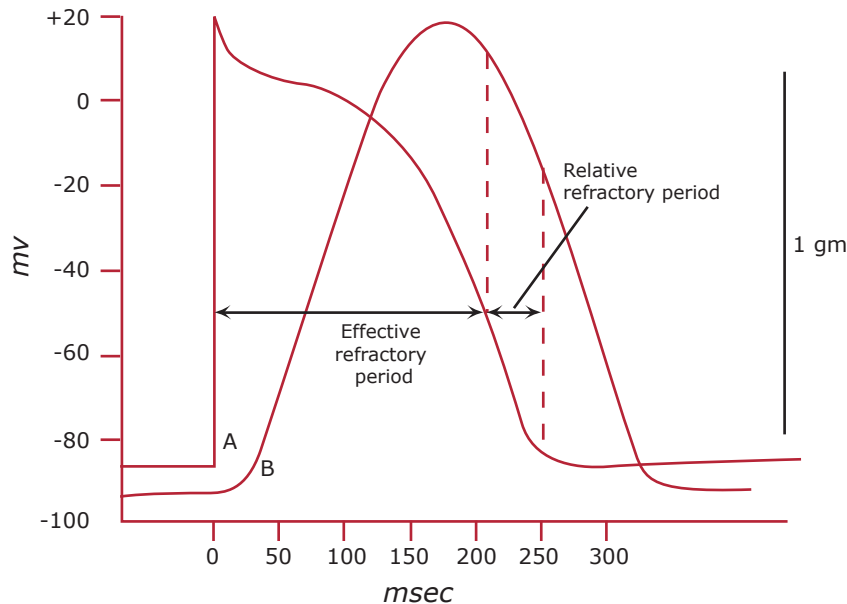


Figure by MIT OCW. After Brooks et al.

1.8 The Cardiac Conduction System

Some muscle cells in the heart are specialized to serve as the “electrical control and distribution system.” They serve to generate periodic impulses which establish the heart rate (pacemaker function), and to rapidly conduct the action potentials to the rest of the heart. Taken as a whole, these cells comprise the cardiac conduction system. The major functional elements include: the sino-atrial (SA) node, the atrioventricular (AV) node, and the intraventricular conduction system. The latter includes the common bundle (Bundle of HIS), the major right and left bundle branches, and the diffusely arborizing which anastomoses with ventricular myocardium. (Recall Fig. 6 which diagrams the anatomy of the conduction system, together with representative transmembrane action potentials.)

The cardiac impulse normally arises in the SA node. This structure is a region of specialized muscle cells located in the right atrium near the entrance of the superior vena cava. Sympathetic and parasympathetic fibers richly innervate this region, and may speed or slow the rate of impulse formation to vary heart rate. Action potentials spread from the SA node throughout the atria with a propagation velocity of about 1 meter/second. Electrophysiologic studies have suggested the existence of at least three routes of preferential conduction in the atria with propagation velocities somewhat greater than in non-specialized atrial tissue. Although some workers doubt the existence of specific anatomically differentiated bundles, they are often referred to as the internodal tracts, and serve to channel the impulse from the SA node to the atrio-ventricular (AV node). Cells in the internodal tracts may also function as pacemakers under the right conditions.

The AV node, or more properly, the AV “junction” is normally the only conducting bridge between atria and ventricles. The electrophysiology of the AV junction is particularly complex. The area has been divided into three regions: the AN region at the atrial end, the N region in the center of the node, and the NH region where the node merges into the common bundle of His (Fig. 19). The velocity of the action potential slows drastically during its passage through the AV junction—particularly in the N region—to 0.02 - 0.05 meters/second. An effective delay of about 70-80 milliseconds is introduced in this manner, thus permitting atrial contraction to be completed before ventricular contraction begins. The AV junction is also richly innervated with autonomic fibers which modulate the conduction velocity. (Increased vagal tone decreases velocity, while increased sympathetic tone increases velocity.) Cells in the AV junction - particularly those in the AN and NH regions - possess the property of autorhythmicity, and many function as the cardiac pacemaker site if impulses fail to reach the area from higher levels in the conduction system.

Figure 19 - Atrioventricular conduction system.

The AV node can be divided functionally into three regions: AN (upper, or atrionodal), N (middle, or nodal), and NH (lower, or nodal-His bundle). (From Katz, Arnold M., *Physiology of the Heart* (New York: Raven Press Books, 1992), p. 467.)

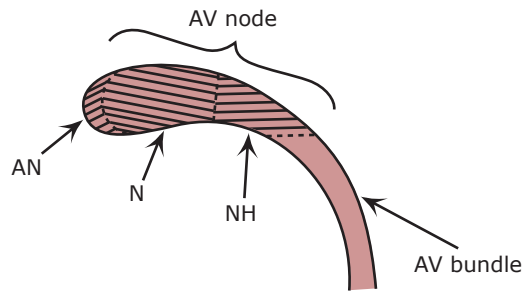


Figure by MIT OCW. After Katz, Arnold M. *Physiology of the Heart*. New York: Raven Press Books, 1992. p. 467.

After emerging from the AV node, the impulse enters the common bundle of His and propagates rapidly at a velocity of 1-2 meters/sec. Activation spreads into the right bundle branch and the two fascicles (anterior and posterior divisions) of the left bundle branch (Fig. 20). Depolarization spreads rapidly (2-4 m/sec.) through the Purkinje system to the muscle cells of the inner wall of the heart. The ventricular muscle cells then continue to conduct the action potential (somewhat more slowly at 0.5-1 m/sec.) from cell to cell, until the entire ventricular muscle mass is depolarized.

Ventricular depolarization begins on the left side of the interventricular septum, spreads to the apex, then to the walls of the ventricles, and finally to the base of the left ventricle. It takes about 80 milliseconds to completely depolarize the ventricles. Fig. 21 illustrates the normal sequence of ventricular depolarization.

Figure 20 - The Ventricular Conduction System

(From Goldman, M.J., Principles of Clinical Electrocardiography, 8th ed., (Lange Medical Publications, 1973), p. 37.)

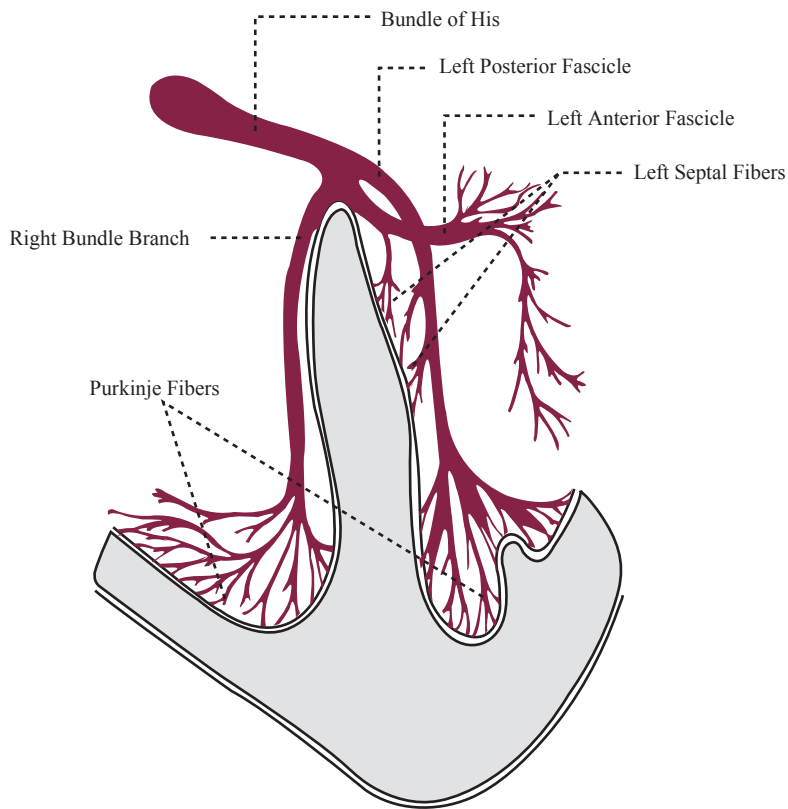


Figure by MIT OCW. After M. J. Goldman, *Principles of Clinical Electrocardiography*. 8th ed (1973), p. 37.

Figure 21 - The normal sequence of ventricular depolarization

The instantaneous heart vector is shown at four times during the process: 10, 20, 40, and 60 milliseconds. (From Massie and Walsh, 1960.)

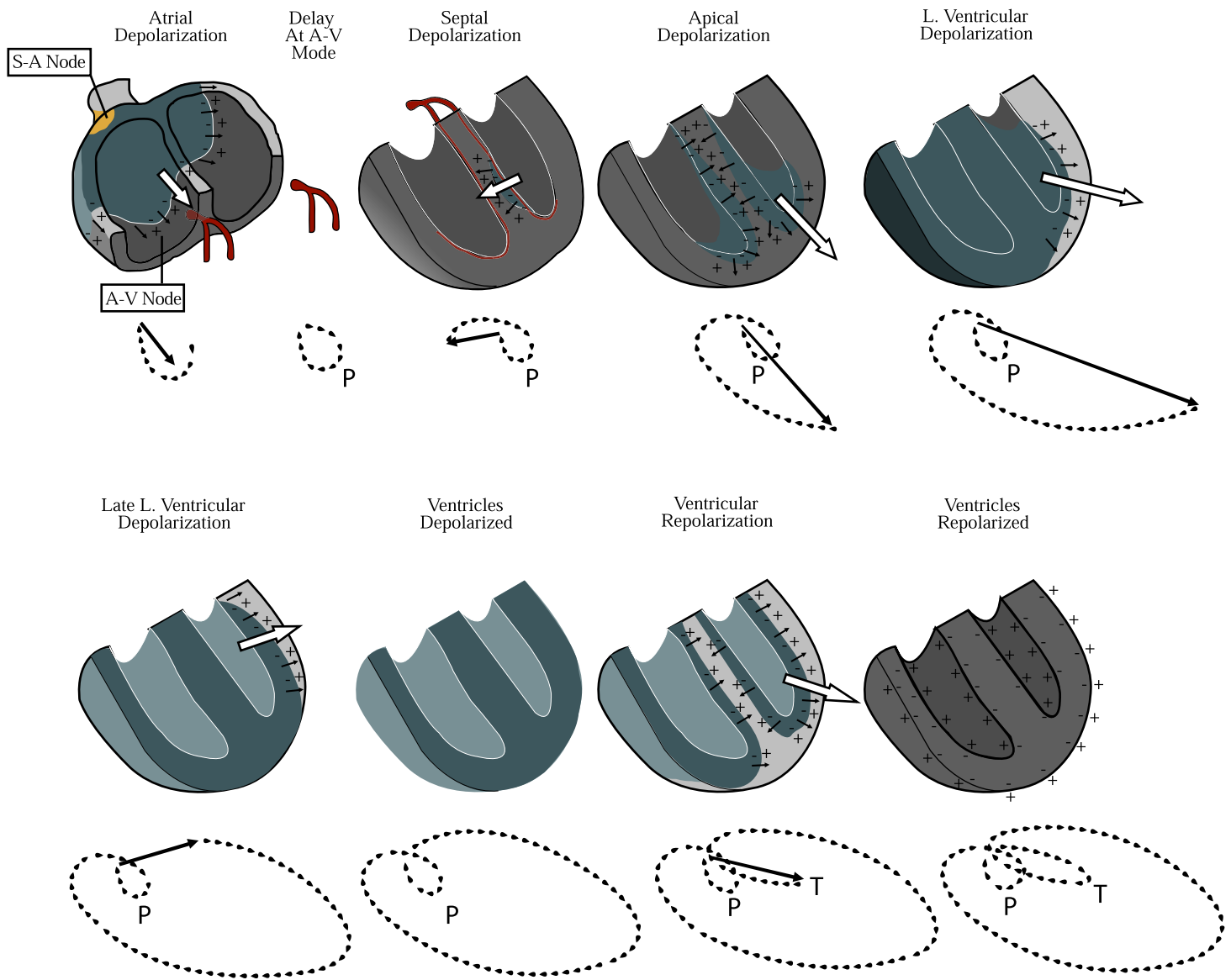


Figure by MIT OCW. After F. Netter.

2. THE PHYSICAL BASIS OF ELECTROCARDIOGRAPHY

2.1 Introduction

In the preceding section, we reviewed the electrophysiology of myocardial cells. As a result of the electrical activity of those cells, current flows within the body and potential differences are established on the surface of the skin which can be measured using suitable equipment. The graphical recording of these body surface potentials as a function of time produces the electrocardiogram (ECG). Fig. 22 illustrates a single-lead scalar electrocardiogram.

Figure 22 - Example of a Scalar Electrocardiogram

(From Philips and Feeney, *The Cardiac Rhythms: A Systematic Approach to Interpretation*, Philadelphia: W.B.Saunders, 1980, p. 36.)



Figure courtesy of PhysioNet (<http://www.physionet.org>).

In this section we wish to examine the relationship between the cellular events and the body surface potentials. The clinician who uses the electrocardiogram as a diagnostic test wishes to determine cardiac abnormalities from the body surface potentials. Given a distribution of body surface potentials, can we specify the detailed electrophysiologic behavior of the source? Unfortunately this “inverse” problem does not have a unique solution as demonstrated in 1853 by Hermann von Helmholtz. It is not, in general, possible to uniquely specify the characteristics of a current generator from the external potential measurements alone.

The “forward” problem is more tractable: given knowledge of the heart generator, can the body surface potentials be specified? If the transmembrane potentials of all the cells within the heart were known, can a mathematical expression be found to specify the extracellular potentials everywhere in the surrounding space? A complete solution would include details of tissue geometry

and electrical properties, as well as an exhaustive description of the detailed electrical activity of the heart. The investigation of the forward problem has frequently employed the use of physical and/or mathematical models. A number of investigators have studied models of the human torso in which they have imbedded well-defined electrical sources. The models are typically plastic containers shaped in the form of a human torso and filled with a conductive liquid medium. Inhomogeneities of the conducting media (such as lungs) are sometimes modeled by bags of lower conductivity material such as sand. By placing well-defined electrical dipole sources within the model torso, the relationship between the cardiac generator and body surface potentials may be studied. Mathematical models have been proposed as well. The heart is typically represented by a number of spatially distributed dipole sources imbedded in a conductive medium of variable complexity. Computer simulations have made it possible to develop impressive demonstrations using hundreds of dipoles, and synthesizing the resultant body surface potential distributions (Miller, Geselowitz, 1978). The simplest mathematical model for relating the cardiac generator to the body surface potentials is the single dipole model. This simple model is an interesting and useful one which dates back to the earliest days of human electrocardiography. It is still extremely useful in providing a framework for the study of clinical electrocardiography and vectorcardiography.

2.2 The Dipole Model

The model has two components: a) a representation of the electrical activity of the heart cells, and b) a representation of the geometry and electrical properties of the body. Having modeled the source and the conductive body media, it is a straightforward task to develop the relationship between source and surface potentials.

2.2.1 The Source

The smallest unit contributing to the ECG is the single myocardial cell. Fig. 23 shows such a cell in which an action potential is propagating. The action potential is associated with a current, $i(x,t)$, within the cell flowing in the direction of propagation of the action potential. The cable model

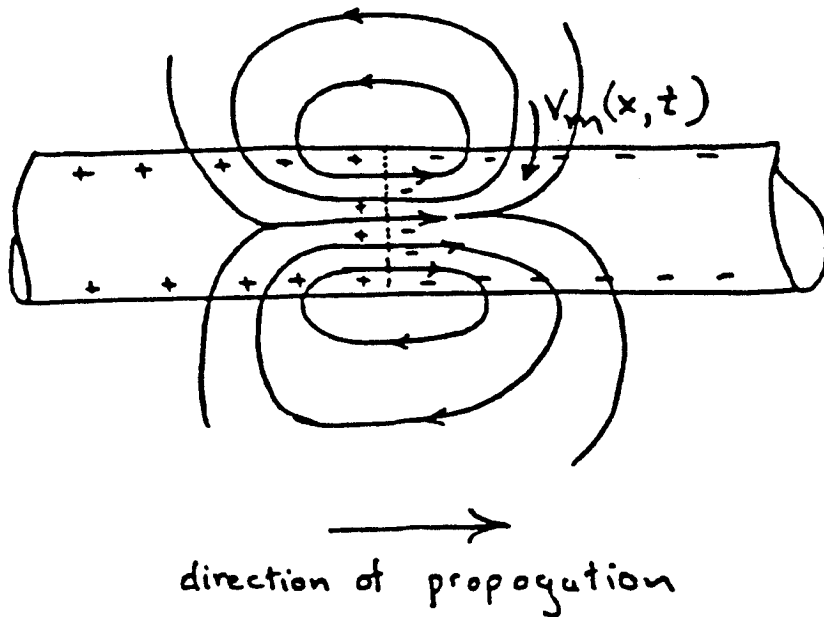
related this current to the spatial gradient of the membrane potential in equation (10) which is rewritten here:

$$i(x, t) = -\frac{1}{(r_i + r_o)} \cdot \frac{\partial V_m(x, t)}{\partial x} \quad (10)$$

If the action potential propagates with constant shape and at constant velocity, c , then it can be shown that $V_m(x, t) = V_m(x - ct)$. It follows that:

$$\frac{\partial V_m(x, t)}{\partial x} = -\frac{1}{c} \frac{\partial V_m(x, t)}{\partial t} \quad (15)$$

Figure 23 - Current flow in a Myocardial Cell at the Advancing Front of Depolarization



Thus, equation (10) may be written

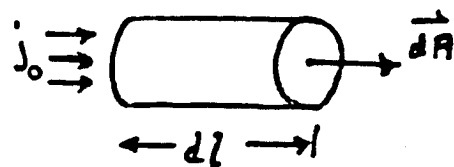
$$i = \frac{1}{(r_i + r_o)} \cdot \frac{1}{c} \cdot \frac{\partial V_m(x, t)}{\partial t} \quad (16)$$

where the variables are defined as in section 1.3.

We will consider the intracellular longitudinal current at the interface of normal and depolarized tissue to be the elementary electrical source, which we will refer to as a ***current dipole***.

A current dipole is an unusual concept, and is worth discussing more carefully. It is defined as a uniform current density, j_o , flowing in a small cylindrical region of length dl , and cross-sectional area dA . (See Fig. 24.) The current flows parallel to $d\vec{A}$ where $d\vec{A}$ is a vector normal to the elemental area dA .

Figure 24 - A Current Dipole



As dA and dl approach zero, the product $(j_o \cdot d\vec{A} \cdot dl)$ remains constant. We will define $\dot{\vec{m}}_o$ as the current dipole moment:

$$\dot{\vec{m}}_o = j_o \cdot d\vec{A} \cdot dl \quad (17)$$

Note that $\dot{\vec{m}}_o$ is a vector quantity and has units of current \times length.

The direction of $\dot{\vec{m}}_o$ points in the direction of propagation of the action potential. If the cell rests in a uniform conducting medium, the current lines will close to form a dipole current field. The assumption that dA and dl approach zero is reasonable in the context of the typical dimensions involved. Myocardial cell diameters are about 10 microns (10^{-3} cm) and typical dimensions of the heart and chest are in the order of tens of centimeters.

It is useful to assign typical numerical values to the intracellular longitudinal current and the corresponding dipole moment given equations (14) and (15) respectively. The action potential amplitude is typically 100 mV, and the rise-time is about 1 millisecond. Thus,

$$\frac{\partial V_m}{\partial t} = 100 \text{ volts/ second}$$

The velocity of propagation is roughly 100 cm/sec. in ventricular muscle. For simplicity we will assume that $r_0 \ll r_i$. The resistance per unit length of the intracellular media, r_i , can be estimated by assuming a resistivity, ρ , of 100 ohm-cm, and a cellular cross-sectional area of approximately 10^{-6} cm^2 . It follows that

$$r_i = \rho/da = 10^8 \text{ ohms/cm}$$

The intracellular current then becomes

$$i = 10^{-8} \text{ amperes}$$

In order to calculate the magnitude of the dipole moment, m_o , we require an estimate of dl , the effective length of the source. Using the previous values of action potential velocity and upstroke time, the estimate for dl is 10^{-1} cm . Thus, the estimated magnitude of the dipole moment would be:

$$|m_o| \approx 10^{-9} \text{ amp-cm}$$

The heart's total electrical activity at any instant of time may be represented by a distribution of active current dipoles. In general, they will lie on an irregular surface corresponding to the boundary between depolarized and polarized tissue.

If the heart were suspended in a homogeneous isotropic conducting medium, and were observed from a distance large compared to its size, then all of the individual current dipoles may be assumed to originate at the same point in space. The total electrical activity of the heart may then be represented as a *single* equivalent dipole whose magnitude and direction is the vector summation of all the individual dipole sources. The net equivalent dipole moment, \dot{M} , is commonly referred to as

the “heart vector”. As cardiac depolarization spreads, the heart vector, $\dot{\vec{M}}$ changes in magnitude and direction as a function of time. (Refer to Fig. 21 above.)

2.2.2 Electrical Properties of Tissue

The sources that characterize the electrical activity of the heart are immersed in the body, and the resulting distribution of currents and potentials depends on the electrical properties of the torso. These have been investigated and the following results have been determined.

Linearity: For the current densities produced by the heart, the body tissues may be considered linear: that is, the potential gradient or electric field is everywhere proportional to the current density.

$$\dot{\vec{J}} = \sigma \dot{\vec{E}} = -\sigma \dot{\nabla} \Phi \quad (18)$$

where $\dot{\vec{J}}$ \equiv current density, σ \equiv conductivity of the tissue, $\dot{\vec{E}}$ \equiv electrical field, and Φ \equiv potential.

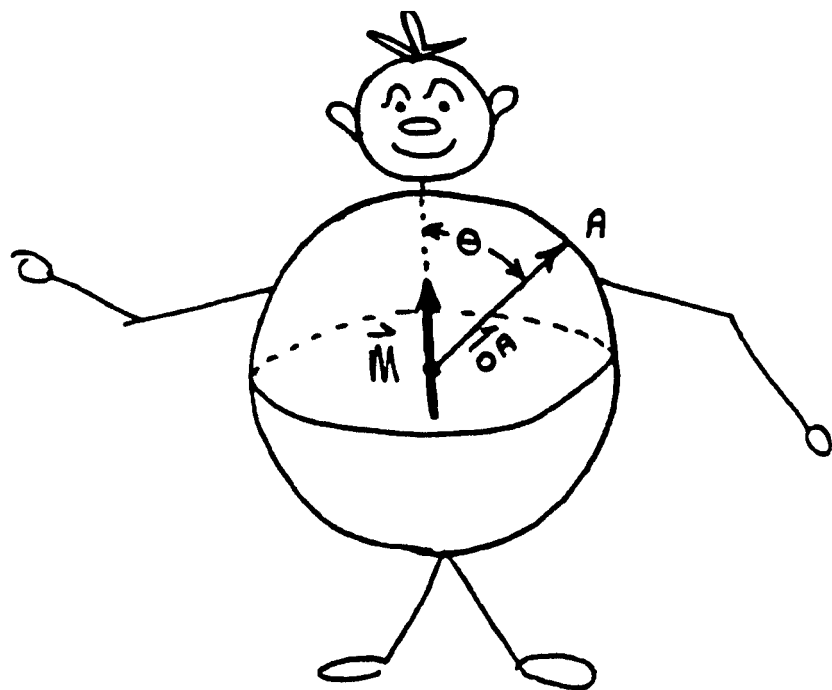
Homogeneity: Different tissues have conductivities which vary considerably from one another. For example, blood has a conductivity approximately five times as great as other tissues, and blood masses such as those within the ventricles and great vessels certainly introduce time-varying inhomogeneities into the thorax. Likewise, lung tissue, although its average conductivity is similar to other tissue, varies by a factor of five or so with respiration! Thus, the torso is far from a homogeneous medium. Furthermore, its properties vary with time!

Anisotropy: An isotropic medium is one in which the properties are independent of orientation or direction. Some tissues are reasonably isotropic in small regions, but not all. In muscle, for example, the impedance along fibers is less than that measured across fibers. In addition, the presence of structures such as high-conductivity cylindrical blood vessels, and low-conductivity bronchi and bone make the thorax a highly anisotropic medium.

Complex Impedance: In the frequency band of interest (0.1 - 10³ Hz), the reactive components of tissue impedance are sufficiently small that the chest may be considered purely resistive.

For simplicity, the dipole model ignores the known anisotropy and inhomogeneity of the torso, and represents it as a linear, isotropic, homogeneous, spherical conductor of radius, R , and conductivity, σ . The source is represented as a slowly time-varying current dipole, \hat{M} , located at the center of the sphere (Fig. 25). The problem is considered as a quasi-static one. The static electric field, current density, and electric potential everywhere within the torso (and on its surface) will be related to the heart vector, \hat{M} .

Figure 25 - The Idealized Spherical Torso with the Centrally Located Cardiac Source



2.2.3 Calculation of Potential within the Sphere

Within the sphere, equation (18) must hold. In addition, since there is no net generation of charge anywhere,

$$\vec{\nabla} \cdot \vec{J} = 0 \quad (19)$$

By combining equations (18) and (19), Laplace's equation for the potential is obtained:

$$\nabla^2 \cdot \Phi = 0 \quad (20)$$

By linearly combining general solutions to Laplace's equation for a sphere in order to satisfy the boundary conditions, the potential field may be found. The boundary conditions are:

1. The potential gradient in the radial direction must be zero at the surface of the sphere, since no current is permitted to flow across the skin into air. Thus,

$$\frac{\partial \Phi(r, \theta)}{\partial r} = 0 \text{ at } r = R \quad (21)$$

2. We have assumed the source to be modeled by an equivalent current dipole of magnitude, M_o , located at the center of the sphere. Hence, from the definition of equation (17), we must have:

$$M_o = \iiint \vec{J} \cdot d\vec{A} dl \quad (22)$$

One solution to Laplace's equation is:

$$\Phi_1(r, \theta) = \frac{K \cos \theta}{r^2} \quad (23)$$

The current densities may be obtained from the potential by using equation (18). Then, using appropriate mathematical manipulations, the integration of equation (22) may be done in the region of the source to evaluate K. The result yields:

$$\Phi_1(r, \theta) = \frac{M_o}{4\pi\sigma r^2} \cos \theta \quad (24)$$

This solution, however, cannot satisfy the first boundary condition at the surface of the sphere (eq. 21). We must add another solution to Laplace's equation of the form:

$$\Phi_2(r, \theta) = Ar \cos \theta \quad (25)$$

Note that this potential disappears at $r = 0$, and thus will not alter our solution for K . The new solution becomes:

$$\Phi(r, \theta) = \Phi_1(r, \theta) + \Phi_2(r, \theta)$$

The boundary condition of eq. (21) is satisfied when

$$A = \frac{2M_o}{4\pi\sigma R^3} \quad (26)$$

Hence, the final solution for the potential within the sphere is:

$$\Phi(r, \theta) = \frac{M_o}{4\pi\sigma} \cos \theta \left[\frac{1}{r^2} + \frac{2r}{R^3} \right] \quad (27)$$

2.2.4 The Surface Potentials

At the surface of the sphere (corresponding to the skin surface on the spherical torso), $r=R$ and

$$\Phi(R, \theta) = \frac{3M_o}{4\pi\sigma R^2} \cos \theta \quad (28)$$

where M_o is the magnitude of the equivalent heart vector, R is the radius of the sphere, and θ is the angle between the point of observation and the direction of the heart vector.

Note that (28) could also be written in vector form

$$\Phi_A = \vec{r} \cdot \vec{M} \bullet \vec{OA} \quad (29)$$

where \overrightarrow{OA} is a vector from the origin to point A on the surface of the sphere, making an angle θ with the axis of the dipole (Fig. 26). The units of \vec{M} are current \times length and the units of \overrightarrow{OA} are ohms/length.

The amplitude of OA is given by:

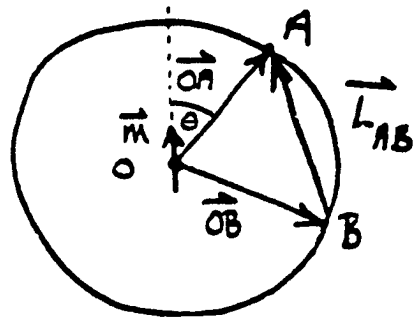
$$|OA| = \frac{3}{4\pi} \cdot \frac{1}{\sigma} \cdot \frac{1}{R^2}$$

Note that this amplitude is determined by the electrical conductance of the medium, σ , and the physical distance, R. As the radius gets larger $|OA|$ becomes smaller, etc. The locus of the tips of \overrightarrow{OA} for all θ forms a surface called an “image surface”. Each point on the torso surface maps into a corresponding point on the image surface. \overrightarrow{OA} is a transfer impedance vector (impedance/length) or a “lead vector”. Eq. (29) thus is a statement of Ohm’s Law.

Referring to Fig. 26, note that the potential at a different point on the surface, B, would be given by:

$$\Phi_B = \vec{M} \bullet \overrightarrow{OB}$$

Figure 26 - Lead Vectors and the Heart Vector



Thus, the potential *difference* between points A and B would be:

$$\begin{aligned}
 V_{AB} &= \Phi_A - \Phi_B = \vec{M} \cdot \vec{OA} - \vec{M} \cdot \vec{OB} \\
 &= \vec{M} \cdot \left(\vec{OA} - \vec{OB} \right) \\
 &= \vec{M} \cdot \vec{L}_{AB}
 \end{aligned}$$

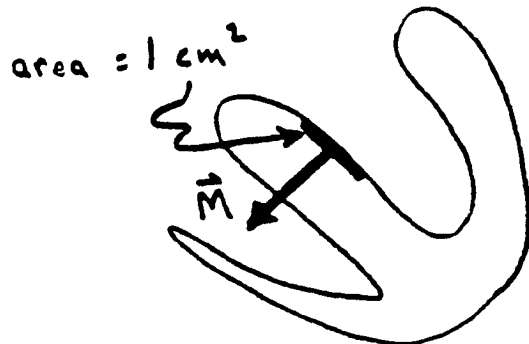
The potential difference V_{AB} is simply the scalar product of the heart vector with vector, \vec{L}_{AB} , which is commonly referred to as the “lead vector”. The lead vector connects the points A and B on the image surface.

Since in general \vec{M} is a function of time, the scalar potential difference V_{AB} will also vary with time. At any instant V_{AB} will be the dot product, or projection of the instantaneous heart vector on lead vector \vec{L}_{AB} .

A wide variety of lead vectors may be formed by attaching electrodes to the body in various positions. This subject will be covered in the next section.

An order-of-magnitude calculation may be made using equation (28) to estimate the value of the body surface potential to be expected from the electrical activity of the heart. We will consider a particular instant during cardiac depolarization when the interface between polarized and depolarized tissue is 1 cm^2 , and is approximately planar (Fig. 27).

Figure 27 - Schematic diagram showing a 1-cm^2 area of interface between polarized and depolarized tissue early in the cardiac cycle.



Since the cross-sectional area of individual cellular dipoles is 10^{-6} cm 2 , there will be approximately 10^6 of them in the interface region, and they will be parallel. Thus, the magnitude of net equivalent heart dipole will be:

$$|M_o| = n|M_o| = 10^6 \times 10^{-9} = 10^{-3} \text{ amp. cm.}$$

We will assume a torso with a radius of 20 cm. and a conductivity, σ , of 3×10^3 ohm $^{-1}$ -cm $^{-1}$. The maximum surface potential would be

$$\Phi_{\max} = \frac{3M}{4\pi\sigma R^2} = 0.2 \text{ mV}$$

Thus, the model predicts surface potentials in the order of fractions of millivolts, which corresponds closely to experimentally measured values early in the sequence of ventricular depolarization.

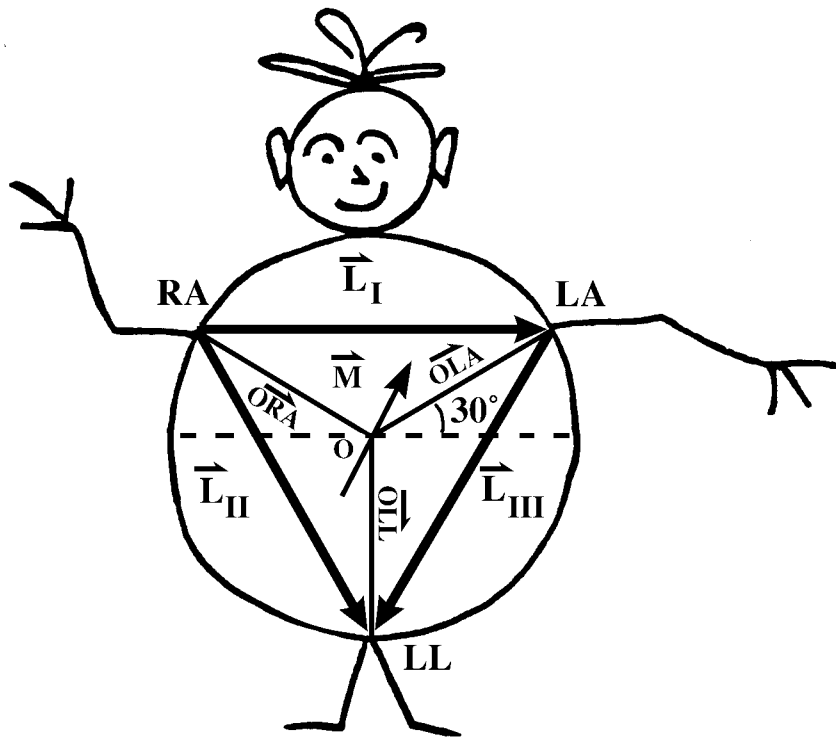
2.3 Lead Systems Used in Scalar Electrocardiography

Not surprisingly, the lead systems used in clinical practice utilize the limbs, since they are convenient point of attachment for electrodes. In addition, chest electrodes are used to record projections of the heart vector onto the horizontal plane.

2.3.1 Frontal Plane Scalar Leads

Suppose an electrode were attached to each arm and one leg of the subject (Fig. 28).

Figure 28 — The Ideal Torso and Dipole Model



The potentials at the points indicated will be:

$$\begin{aligned}\Phi_{RA} &= \vec{M} \cdot \vec{ORA} \\ \Phi_{LA} &= \vec{M} \cdot \vec{OLA} \\ \Phi_{LL} &= \vec{M} \cdot \vec{OLL}\end{aligned}\tag{33}$$

The potential differences between the limb leads may also be determined. In electrocardiography the standard limb lead voltages are defined as:

$$\begin{aligned}V_I &= \Phi_{LA} - \Phi_{RA} \\ V_{II} &= \Phi_{LL} - \Phi_{RA} \\ V_{III} &= \Phi_{LL} - \Phi_{LA}\end{aligned}\tag{34}$$

From our previous considerations, and noting the definition of lead vectors \dot{L}_I , \dot{L}_{II} , and \dot{L}_{III} from Fig. 28, we have:

$$\begin{aligned} V_I &= \overset{r}{M} \bullet \left(\overrightarrow{OLA} - \overrightarrow{ORA} \right) = \overset{r}{M} \bullet \dot{L}_I \\ V_{II} &= \overset{r}{M} \bullet \dot{L}_{II} \\ V_{III} &= \overset{r}{M} \bullet \dot{L}_{III} \end{aligned}$$

A simple way to visualize these results is to note that V_I is simply the projection of the heart vector \dot{M} on the lead vector \dot{L}_I .

It has been found useful in electrocardiography to define a “central terminal” by averaging the potentials from the limb leads.

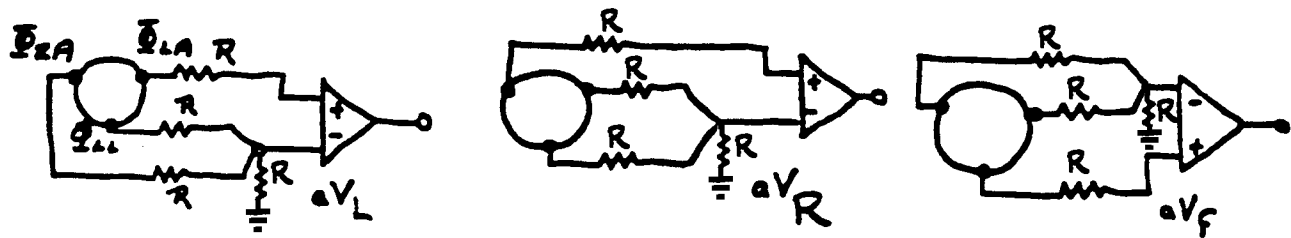
$$\begin{aligned} \Phi_{CT} &= \Phi_{RA} + \Phi_{LA} + \Phi_{LL} \\ &= \overset{r}{M} \bullet \left(\overrightarrow{ORA} + \overrightarrow{OLA} + \overrightarrow{OLL} \right) \\ &= 0 \end{aligned}$$

since the vectors in the parenthesis sum to zero. Using the central terminal as a reference, one may now construct new lead vectors

$$\begin{aligned} V_L &= \Phi_{LA} - \Phi_{CT} = \Phi_{LA} = \overset{r}{M} \bullet \overrightarrow{OLA} \\ V_R &= \Phi_{RA} = \overset{r}{M} \bullet \overrightarrow{ORA} \\ V_F &= \Phi_{LL} = \overset{r}{M} \bullet \overrightarrow{OLL} \end{aligned} \tag{37}$$

These leads may be improved by using the circuits shown in Fig. 29.

Figure 29 — Standard Connections for Augmented Limb Leads



$$\begin{aligned}
 aV_L &= \Phi_{LA} - \left[\frac{\Phi_{RA} + \Phi_{LL}}{2} \right] = 1.5V_L \\
 aV_R &= \Phi_{RA} - \left[\frac{\Phi_{LA} + \Phi_{LL}}{2} \right] = 1.5V_R \\
 aVF &= \Phi_{LL} - \left[\frac{\Phi_{LA} + \Phi_{RA}}{2} \right] = 1.5V_F
 \end{aligned} \tag{38}$$

These leads are referred to as the *augmented limb leads*.

The complete set of frontal lead vectors is shown in Fig. 30 with all vectors drawn to pass through the origin. It should be noted that the amplitudes of these lead vectors are not equal. $\dot{L}_I, \dot{L}_{II}, \dot{L}_{III} = R\sqrt{3}$ while the augmented leads are $1.5R$. (This difference will be ignored.)

2.3.2 Precordial Leads

By using the “central terminal” as a reference electrode, and placing an exploring electrode at various points on the chest, a variety of horizontal plane lead vectors may be obtained. In clinical practice, six standard chest leads are used, and are termed V_1, V_2, \dots, V_6 . The placement of the electrodes is shown in Fig. 31.

A complete scalar ECG, then, would consist of 12 leads - six frontal plane and six precordial leads.

Figure 30 — Frontal Plane Limb Leads

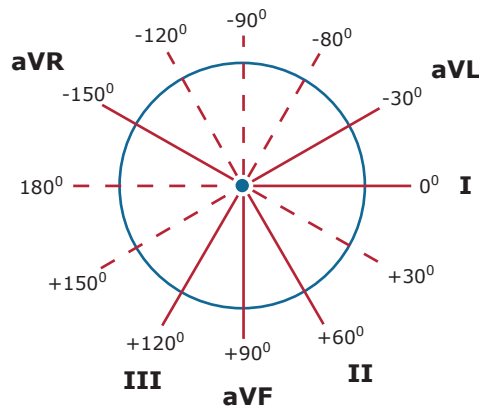


Figure by MIT OCW.

Figure 31 — The Six Standard Chest Leads

The location of these leads is as follows:

V₁: on the fourth intercostal space at the right sternal margin

V₂: on the fourth intercostal space at the left sternal margin

V₃: midway between leads V₂ and V₄

V₄: on the fifth intercostal space at the midclavicular line

V₅: on the anterior axillary line at the horizontal level of lead V₄

V₆: on the midaxillary line at the horizontal level of lead V₄

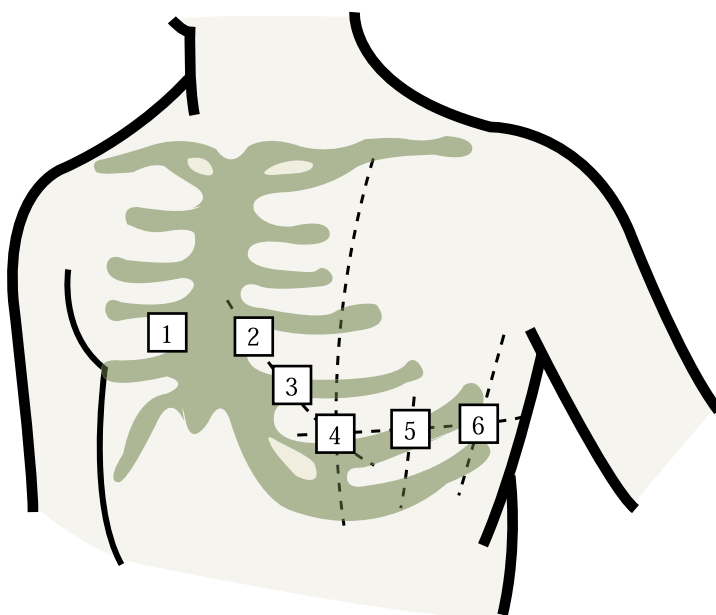


Figure by MIT OCW.

2.4 Electrical Axis

The complete description of the source is a three-dimensional plot of the locus of the tip of the equivalent heart vector. The same information could be presented in three two-dimensional plots showing the projection of the locus on the horizontal, frontal, and sagittal planes. This type of display is termed the *vectorcardiogram*. A typical frontal-plane loop is illustrated in Fig. 32.

Figure 32 — A Frontal Plane VCG Loop

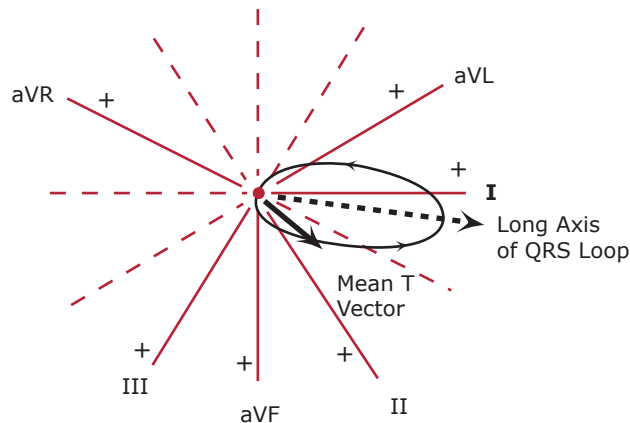


Figure by MIT OCW.

A waveform that would be recorded on lead I of the scalar ECG is simply the plot of the projection of the loop onto \hat{L}_I as a function of time. Similarly, the waveform that would be seen in Lead II is the projection of the loop onto \hat{L}_{II} . These plots are shown in approximate form in Fig. 33.

Figure 33 - Scalar Projections of the VCG on Limb Leads I, II, and III

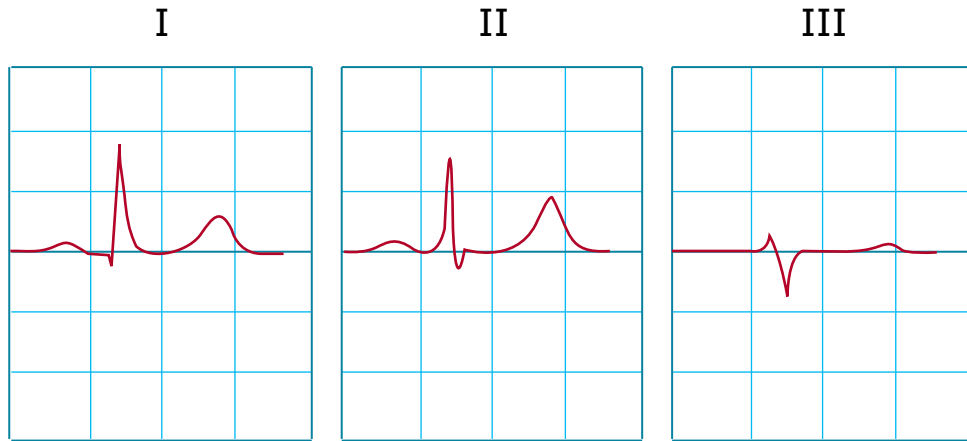
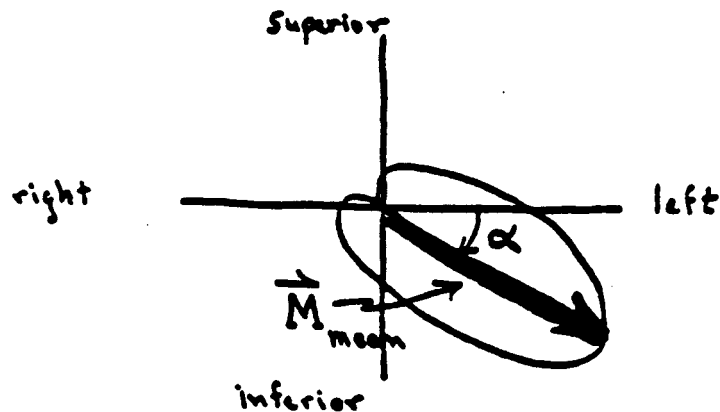


Figure by MIT OCW.

The vector loop shown in Fig. 32 could be thought of as the locus of the tips of many individual vectors, each of which is an instantaneous equivalent cardiac vector occurring at a different time. The angle that each such vector makes with the horizontal would then correspond to the instantaneous electrical axis of the heart in the *frontal plane*. The instantaneous axis of greatest magnitude is the major instantaneous axis of the heart. Of more importance clinically is the *mean electrical cardiac vector*. This represents the mean magnitude and direction of all the instantaneous vectors. The *mean electrical axis* of the heart is that angle, α , that the mean vector makes with the horizontal (see Fig. 34). Note that angles are measured *clockwise* clinically, starting from the horizontal. Normal axes fall between -10° and $+110^\circ$.

Figure 34 — The Mean Electrical Cardiac Vector



Mathematically, we may represent the instantaneous equivalent cardiac vector as projected in the frontal plane as $\dot{\vec{M}}(t)$. The mean vector is then:

$$\overset{r}{\vec{M}}_{\text{mean}} = \frac{\dot{\vec{M}}(0) + \dot{\vec{M}}(\Delta t) + \dots + \dot{\vec{M}}(n\Delta t)}{n+1} \quad (39)$$

This vector addition may be broken up into scalar components using any two lead vectors, which we will represent by $\overset{\perp}{\vec{L}}_A$ and $\overset{\perp}{\vec{L}}_B$.

$$\overset{\perp}{\vec{M}}_{\text{mean}} = \overline{V}_A \overset{\perp}{\vec{L}}_A + \overline{V}_B \overset{\perp}{\vec{L}}_B \quad (40)$$

where \overline{V}_A is the magnitude of the projection of $\overset{\perp}{\vec{M}}_{\text{mean}}$ onto the lead vector $\overset{\perp}{\vec{L}}_A$, and likewise for \overline{V}_B . Thus,

$$\begin{aligned}\overline{V}_A &= \overset{\perp}{\vec{M}}_{\text{mean}} \bullet \overset{\perp}{\vec{L}}_A \\ \overline{V}_B &= \overset{\perp}{\vec{M}}_{\text{mean}} \bullet \overset{\perp}{\vec{L}}_B\end{aligned}$$

It follows that

$$\begin{aligned}\overline{\vec{M}}_{\text{mean}} &= \left[\frac{V_A(0) + V_A(\Delta t) + V_A(2\Delta t) + \dots + V_A(n\Delta t)}{n+1} \right] \overset{r}{\vec{L}}_A + \\ &\quad \left[\frac{V_B(0) + V_B(\Delta t) + V_B(2\Delta t) + \dots + V_B(n\Delta t)}{n+1} \right] \overset{r}{\vec{L}}_B\end{aligned}$$

By letting $\Delta t \rightarrow 0$ and $n \rightarrow \infty$ while keeping $n\Delta t = T$, multiplying numerators and denominators by Δt , and substituting integrals for sums, the following is obtained:

$$\overset{r}{\vec{M}}_{\text{mean}} = \left[\frac{1}{T} \int_0^T V_A(t) dt \right] \overset{r}{\vec{L}}_A + \left[\frac{1}{T} \int_0^T V_B(t) dt \right] \overset{r}{\vec{L}}_B \quad (43)$$

Thus

$$\overline{V}_A = \frac{1}{T} \int_0^T V_A(t) dt \quad (44)$$

$$\bar{V}_B = \frac{1}{T} \int_0^T V_B(t) dt \quad (45)$$

$V_A(t)$ and $V_B(t)$ are simply the scalar projections of $\dot{\bar{M}}$ on $\dot{\bar{L}}_A$ and $\dot{\bar{L}}_B$. They are scalar functions of time (the ECG). The time, T , is the duration of the QRS complex.

If

$$\dot{\bar{M}}_{\text{mean}} \bullet \dot{\bar{L}}_A = \frac{1}{T} \int_0^T V_A(t) dt = 0$$

then $\dot{\bar{M}}_{\text{mean}}$ must be perpendicular to $\dot{\bar{L}}_A$. This observation allows the clinician to make a rapid estimate of the mean electrical axis of the heart from a quick inspection of the six frontal scalar leads. One simply locates that lead where the mean area under the QRS complex is zero, or nearly so, and concludes that the mean axis of the heart is perpendicular to that lead. The sense of the vector is easily determined by observing the polarity of the net area under the curve of lead I. For example, if this area were positive, the mean axis would have to lie in quadrants I or IV. Thus, in Figs. 32 and 33 above, we see that since

$$\frac{1}{T} \int_0^T V_{\text{III}}(t) dt \approx 0,$$

the mean electrical axis must be perpendicular to lead III: either $+30^\circ$ or -150° . Since $\bar{V}_L > 0$, the mean axis must be $+30^\circ$.

One may approximate areas under the QRS complex by measuring amplitudes only, and assuming equal widths for positive and negative spikes. The net area is then proportional to the sum of all positive peaks in the QRS minus the sum of all negative spikes. In this way, the ratio of any two arbitrary means may be calculated, and the mean axis constructed graphically.